Sensor phenomena

A Miniature pH Sensor in a Subcutaneous Injection Needle for Biofluid Sensing

Khengdauliu Chawang* , Sen Bing* , Jon Stellar*, and J.-C. Chiao[1]**

Department of Electrical and Computer Engineering, Southern Methodist University, Dallas, TX 75206 USA
**Member, IEEE*
***Fellow, IEEE*

Manuscript received 21 July 2024; revised 28 August 2024; accepted 1 September 2024. Date of publication 4 September 2024; date of current version 11 September 2024.

Abstract—The pH value in bodily fluids is a crucial diagnostic marker. Conventional glass-rod pH sensors display reliability in aqueous solutions, but the pH-sensitive glass membrane makes them prone to inaccuracies in viscous solutions due to elevated junction potentials and bulky design hinders miniaturization. To overcome this issue, this work introduces a new pH sensor design and fabrication that enables miniaturization and reliability in aqueous and viscous solutions and facilitates insertion into a needle for in vivo monitoring. Utilizing a printing technique for the application of iridium oxide (IrOx) and silver/silver chloride coating on a single flexible polyimide substrate offers cost-effectiveness and production scalability. The sensor then is tailored with a sharp blade to a narrow strip that fits into a 20-gauge needle. The electrochemical measurements demonstrate that electrodes produced through this method demonstrate an accuracy of up to 0.1 pH within a narrow pH range (7.35–7.45) in buffer solutions and real human serum tests.

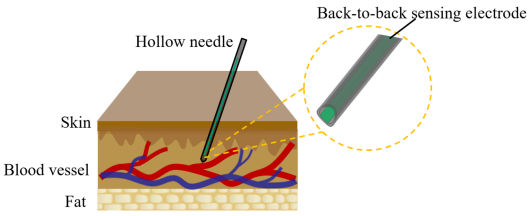

Index Terms—Sensor phenomena, biofluid, flexible, iridium oxide (IrO_x), miniature, pH sensor, printable back-to-back (b2b).

I. INTRODUCTION

The pH value indicates H^+ activity in tissues, which is crucial for health assessment [1]. pH change in body fluid shows metabolic states and is frequently monitored for medical diagnosis. For instance, tumor cells proliferate as the extracellular pH changes from normal pH 7.3 to abnormal pH 6.8 [2] leading to vital organ failure due to an acidic environment [3]. Reports suggest that skin pH changes from a mean acidic pH 4.7 to an alkaline pH 9 in chronic wounds [4]. Inflammatory responses, such as sepsis, require early diagnosis for timely treatment [5]. Therefore, pH sensors are crucial for treatment regulation and early diagnosis [6]. Traditional pH-sensitive glass membranes offer stable pH responses in an aqueous solution, but in viscous fluids, such as blood, protein adsorption causes inaccuracies [7], [8]. Salt bridges can mitigate this effect and prevent contamination, but they are bulky. Recent advances in wearables integrate salt bridges on flexible substrates, but only for skin applications [9], [10]. This letter proposes a pH sensor eliminating the need for salt bridges and enabling miniaturization for needle insertion to conduct fluid pH monitoring in tissues.

Biofluid sensing requires miniature pH electrodes to exhibit biocompatibility, sensitivity in the physiological pH range, and quick response. Although commonly used pH-sensitive materials, such as hydrogen ionophores (HI) and polyaniline (PANI) demonstrate excellent pH characteristics, they raise concerns regarding biocompatibility [11]. Microelectrodes coated with HIs, such as tridodecy-lamine and 4–nonadecylpyridine, are suggested to be biotoxic during direct skin contact [12]. PANI with low-molecular weight benzidine as a byproduct has been studied to be cytotoxic and carcinogenic [13]. Therefore, for a detection platform, these materials are suggested to avoid open skin or tissue contact [14].

Most pH-sensitive metal oxides coated on flexible polyimide substrates show negligible toxicity and allow size scalability [15]. Among these, iridium oxide (IrO_x) stands out for its biocompatibility and inert nature, extensively researched in physiological and microscopic settings [16]. Reports demonstrate that IrO_x possesses desirable properties, such as high charge injection, making it suitable for neural implants without damaging surrounding tissues [17]. Size scalability and substrate flexibility enable continuous blood pH monitoring from veins with a minimal blood sample volume as demonstrated in animal experiments [18]. The Nernstian relationship between potential and pH over a wide pH range [19], biocompatibility [20], quick response in aqueous and nonaqueous solutions [21], and selectivity [22] features make IrO_x an attractive choice for physiological measurement purposes. Common IrO_x deposition includes thermal, radio-frequency magnetron sputtering, and sol–gel processes. While thermal and sputtering methods necessitate vacuum systems, elevating processing costs, sputtered IrO_x films (SIROF) display robust adhesion and have been investigated for neural stimulation [23]. However, the coating process is not economical due to material waste from high-purity target discs. To reduce material waste, recent efforts have been made to create uniform flux and prevent preferential material usage from circular areas [24]. The additional steps to reclaim material waste and vacuum units make the SIROF methods expensive. Sol–gel deposition does not require vacuum systems and waste is minimized since deposition is equal to consumption during film growth. Sol–gel provides good adhesion [25] and the film thickness can be increased by multiple dipping [26]. Our group demonstrated a sol–gel IrO_x film coated on polyimide with a thermal tolerance of 400 °C and the oxide layer

Corresponding author: J.-C. Chiao (e-mail: jchiao@smu.edu).
Associate Editor: Thilo Sauter.
Digital Object Identifier 10.1109/LSENS.2024.3454486

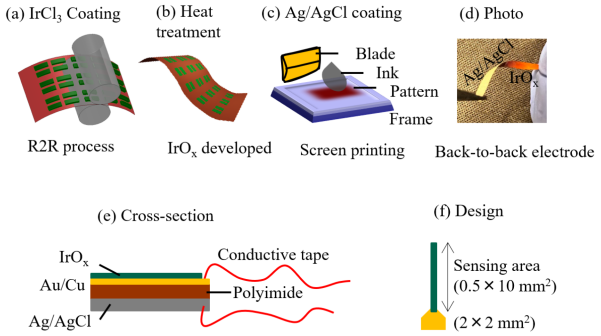

Fig. 1. (a) $IrCl_3$ solution coated on flexible polyimide by R2R process. (b) Coated polyimide heated for IrO_x development. (c) Ag/AgCl ink printed on the other side of polyimide. (d) Electrode photo. (e) Cross-sectional view. (f) Tailored miniature b2b electrode design.

is formed at 325 °C [27], [28], [29]. Previous design was a typical potentiometric pH sensor with two electrodes, one operating as the working electrode and the other as the reference electrode [27], [28], [29]. This letter reports a new design with IrO_x as a working electrode and Ag/AgCl as a reference electrode, both printed back-to-back (b2b) on a single piece of a polyimide film. For applications, the electrode was miniaturized to 0.5 × 10 mm^2 to fit inside a 20-gauge needle for detecting a small fluid volume inside tissues.

Initial measurements, such as open-circuit potential (OCP) and cyclic voltammetry (CV), in buffer showed promising results with test protocols performed with 0.5 and 0.1 pH step changes. Detecting small changes is crucial to identify metabolic state since the blood pH range is 7.35–7.45. Miniature b2b electrodes were further probed into a phantom for monitoring human serum with 0.1 pH changes. Clarke error grid analysis demonstrated the repeatability feature of the sensing electrode.

II. ELECTRODE FABRICATION AND MATERIALS

Flexible polyimide (Sheldahl, USA) was coated with copper and gold layers (18 and 90 nm thick, respectively). Anhydrous iridium (Sigma, USA), ethyl alcohol (Supelco, USA), and 80% acetic acid (Labchem, USA) were mixed for the sol–gel solution. The iridium chloride ($IrCl_3$) solution was coated on the polymeric substrate using a roll-to-roll (R2R) process [29]. The processes are shown in Fig. 1(a)–(c). The substrate was heated at a rate of 1 °C/min, held at 325 °C for 4 h to form IrO_x, and then cooled at −1 °C/min. The Ag/AgCl paste was applied to the backside of the electrode using screen printing. Individual electrode photos and cross-sectional views are provided in Figs. 1(d) and (e). The miniature b2b electrode, designed for probing in a phantom, is shown in Fig. 1(f) with a sensing area of 0.5 × 10 mm^2, and an electrical connection pad of 2 × 2 mm^2.

Custom buffers were made by mixing commercial buffers with 0.05-M sodium chloride (NaCl) salt (Fisher, USA) to enhance solution conductivity. For biological relevance, miniature electrodes were tested in phosphate-buffered saline (1X PBS) (Fisher, USA) with a 0.137-M NaCl concentration [30]. pH levels of PBS were adjusted with hydrochloric acid (HCl) (LabChem, USA) and sodium hydroxide (Sigma-Aldrich, USA). Buffer solution temperatures were monitored with a digital thermometer (Elitech, USA). A commercial pH sensor (Apera, USA) measured human serum pH (Sigma-Aldrich, USA). A phantom with a silicone tube mimicked blood vessels for the body fluid experiments. Electrochemical techniques, including OCP and CV, were conducted using a potentiostat (CH Instrument, USA). The electrical interface and data recording were established using a data acquisition card (National Instruments, USA), controlled by a LabView program, with a sampling rate of 1 S/s.

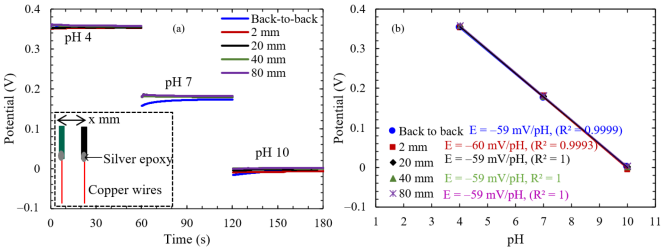

Fig. 2. (a) Potential responses at pH 4, 7, and 10 for a single b2b electrode and single-sided electrodes of IrO_x versus AgCl that are spaced with a distance from 2 to 80 mm. (b) Nernstian response shows b2b fits linearly into the calibration curve. All electrode sizes were 2 × 10 mm^2 for consistent comparison.

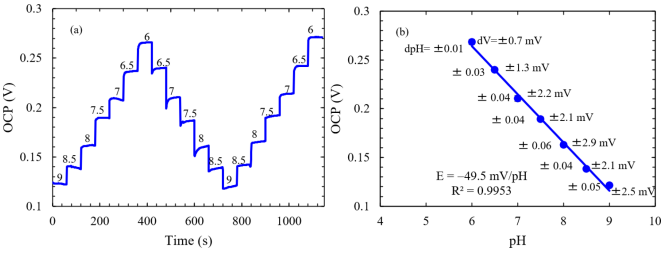

Fig. 3. (a) OCP measurement of a miniature b2b electrode from pH 9 to 6 with 0.5 pH steps. (b) Sensitivity from OCP measurements.

III. RESULTS AND DISCUSSION

A. B2B Design Compared to Two-Electrode Design

The b2b printed electrode was tested in custom buffers and compared to a two-electrode design from previous studies [29]. The inset in Fig. 2(a) illustrates the two-electrode design configuration where IrO_x (green) and Ag/AgCl electrodes (black) are separated by "x" mm distance ranging from 2 to 80 mm. All electrode sizes were 2 × 10 mm^2 and tested in custom-made buffers pH 4, 7, and 10. The electrodes were tested for 60 s in all pH levels. Fig. 2(a) shows that the potential responses for the b2b electrode are consistent with those by two-electrode designs. Fig. 2(b) demonstrates that regardless of electrode spacing, the Nernstian sensitivities of –59 mV/pH are maintained. This shows printing IrO_x and Ag/AgCl b2b does not change the Nernstian responses dramatically.

B. Miniature B2B Electrode in PBS

The b2b electrode was further miniaturized to 0.5 × 10 mm^2, as shown in Fig. 1. For biofluid applications, this electrode was tested in 1X PBS from pH 6 to 9 for biological relevance. All 1X PBS solutions had 0.137-M NaCl salt concentration close to that in typical human body fluid [30]. Fig. 3(a) shows the OCP measurements for 60 s at each pH solution from pH 6 to 9. Electrodes were cleaned in deionized (DI) water between tests. The output potential changed with every 0.5 pH step. The electrode showed a sensitivity of –49.5 mV/pH in Fig. 3(b). The reduced surface area of 0.5 × 10 mm^2 could account for the lower sensitivity, compared to –59 mV/pH of 2 × 10 mm^2 electrodes. Liao and Chou [31] demonstrated that the sensitivity of metal oxide is influenced by the number of hydroxyl groups per unit surface area.

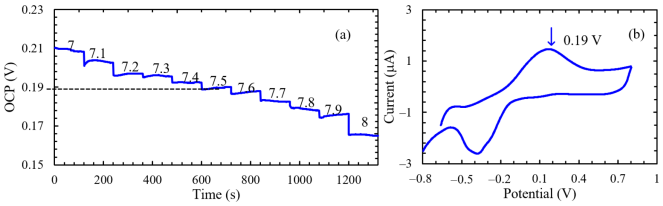

Fig. 4. Electrochemical measurements of a miniature b2b electrode during (a) OCP from pH 7 to 8 with 0.1 pH steps and (b) CV in PBS 1X pH 7.5 with a scan range of −0.8 to + 1 V and a scan rate of 10 mV/s.

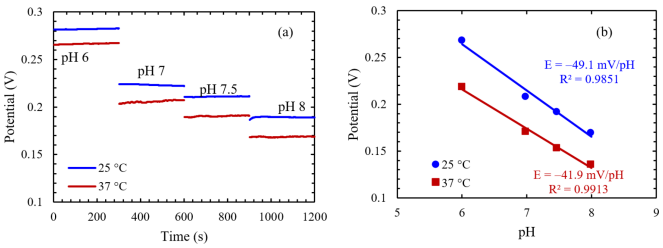

Fig. 5. Miniature b2b electrodes tested at (a) 25 and 37 °C. (b) Corresponding sensitivities.

The miniature b2b electrode demonstrated acceptable hysteresis (dV) and their corresponding pH variation (dpH), as indicated by the error bars in Fig. 3(b). Hysteresis (dV) was previously defined as the standard error of the potential difference at the same pH level [29]. The "±" sign in the dV indicates an average variation between the maxima and minima potentials. Hysteresis was in the range of ±(0.7–2.9) mV with a corresponding pH variation (dpH) range of ±(0.01–0.06) in various aqueous buffer solutions.

Fig. 4(a) shows the miniature b2b electrode tested continuously from pH 7 to 8 without DI cleaning. Each test continued for 120 s and the output potential changed with every 0.1 pH step change. The dotted line at pH 7.5 showed a stable OCP output of 0.19 V comparable to the anodic peak in Fig. 4(b) during the CV measurement. Similar anodic and cathodic enhanced areas illustrate reversible electrochemical mechanisms. For CV, the miniature 0.5 × 10 mm^2 IrO_x was tested against a commercial glass-rod Ag/AgCl electrode and a platinum foil used as reference and counter electrodes, respectively. The CV study using a commercial Ag/AgCl electrode corroborates the stable and repeatable performance of a change to the miniature b2b electrode.

C. Temperature Effect

Fig. 5(a) shows that miniature b2b electrodes were first tested from pH 6 to 8 at the room temperature of 25 °C and then switched to 37 °C. Tests were performed in a 30-mL beaker, and a digital thermometer tracked temperature rise to 37 °C. The electrodes were cleaned in DI water between tests to remove surface residues. The output potential was recorded for 5 min at pH 6, 7, 7.5, and 8. The blue and red lines indicate tests at 25 and 37 °C, respectively. The decreased output potentials at 37 °C are consistent with previous reports [29]. Fig. 5(b) shows the comparable sensitivities of –49.1 and –41.9 mV/pH at 25 and 37 °C. The sensitivities were linear at both temperatures indicated by R^2 values.

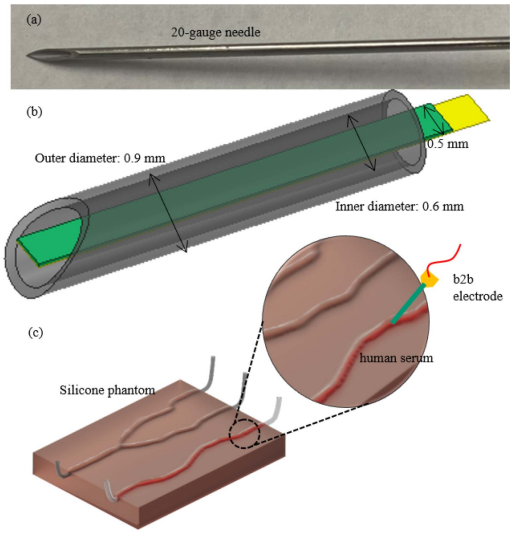

Fig. 6. (a) Photo of a 20-gauge stainless needle. (b) Miniature b2b electrode inside a hollow needle. (c) Blood vessel phantom and illustration of the needle insertion.

D. Miniature B2B Electrode Tested in Human Serum

Fig. 6(a) shows a 20-gauge hollow needle with a size safe for biopsy sampling in clinical practices [32] and Fig. 6(b) illustrates the inner and outer diameters of 0.6 and 0.9 mm, respectively, for the placement of the miniature b2b electrode with a width of 0.5 mm inserted inside the needle. For the fluid tests, Fig. 6(c) shows a silicone phantom with an artificial vessel tube filled with 1 mL of human serum. The needle was used as a guide to allow the interfacing between the miniature b2b electrode and the human serum inside the vessel. The phantom tube diameter of 5 mm is close to that of a forearm vein, while the average vein diameter in the human body is in the range of 7–15 mm [33]. The calculated amount of liquid in contact with the pH probe was 10 μL.

Four different solutions were used: PBS solution with a pH of 7.5, and human sera with pH levels of 7.68, 7.9, and 8. A commercial pH meter measured the commercial human serum as pH 8. The direct addition of concentrated 16.456-M HCl to the serum for pH adjustment led to protein denaturation within the serum, resulting in unreliable and noisy readings. Instead, mixing the PBS solution with the human serum at fixed ratios yielded more stable and accurate results. For instance, mixing the pH 8 serum with a pH 6 PBS solution in a 2:1 ratio resulted in a serum of pH 7.68. Similarly, combining the pH 8 serum with pH 7.5 PBS solution in a 1:1 ratio produced a serum with pH 7.9.

Four newly made miniature b2b electrodes were tested in the four solutions inside the phantom, as shown in Fig. 7. The electrodes showed low potential drift (V') when tested for 1 h. The V' is indicated by the dotted line, which was previously defined as the difference between the initial potential shoot and settled potential [29]. The V' at pH 7.5, 7.68, 7.9, and 8 were 5.6, 1.6, 1.2, and 0.8 mV, respectively. The electrode showed a stable and distinct response to a 0.1 pH step change in human serum. To demonstrate repeatability, three new electrodes underwent ten tests each in sera with pH 7.68, 7.9, and 8. Two calibration methods were employed using data from PBS and serum. The first calibration used the output potentials of PBS at pH 7.5 and serum pH 8 to establish the potential–pH slope. The maximum pH variations from such a calibration were 0.01, 0.01, and 0.05 at pH levels 7.68, 7.9, and 8, respectively. The second calibration method utilized

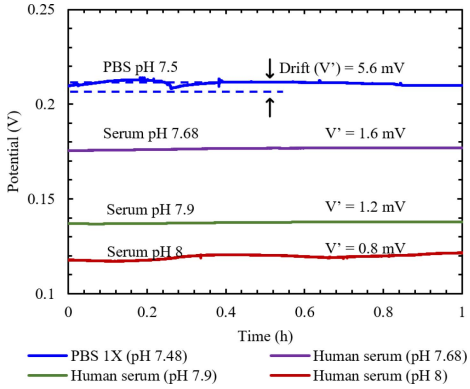

Fig. 7. Potential drift (V') for a miniature b2b electrode inserted inside the blood vessel phantom filled with PBS and human serum.

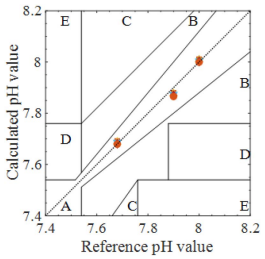

Fig. 8. Repeatability of miniature b2b electrodes tested in human serum shown in a Clarke error grid.

output potentials at pH levels of 7.68, 7.9, and 8 of serum, resulting in reduced variations. After the calibration slope was established, among the subsequent nine tests, the highest pH variations observed were 0.001, 0.03, and 0.002 for tests conducted at pH levels of 7.68, 7.9, and 8, respectively. Fig. 8 shows the pH outputs after the serum calibration was established in a Clarke Error Grid. All nine pH values overlap, indicating an acceptable accuracy.

IV. CONCLUSION

This letter presents a miniature pH sensor fabricated b2b on a flexible polyimide film and tailored into a strip small enough to fit inside a 20-gauge needle. It was designed to detect a small volume of biofluid inside tissues, particularly a blood vessel. The electrode exhibits responsiveness to 0.1 pH variations with repeatability in both buffer solutions and mixed human sera. The ability to detect such subtle pH changes is vital for monitoring human health conditions, given the narrow pH range of human blood (7.35–7.45). The biocompatibility of IrO_x, coupled with its capability to detect small pH changes, renders it a suitable material for clinical diagnostic purposes. Its simple fabrication process and compact size pave the way for potential integration into medical instruments for early detection of blood infections, such as sepsis. The timely identification of sudden pH change is crucial for prompt treatment at the initial stage of infection to avoid catastrophic and potentially deadly outcomes.

ACKNOWLEDGMENT

This work was supported by the School of Engineering at Southern Methodist University, Mary and Richard Templeton Endowment.

REFERENCES

[1] S. Lim, "Metabolic acidosis," *Acta Med Indones*, vol. 39, pp. 145–150, 2007.
[2] X. Zhang, Y. Lin, and R. J. Gillies, "Tumor pH and its measurement," *J. Nucl. Med.*, vol. 51, pp. 1167–1170, 2010.
[3] A. U. Alam et al., "Polymers and organic materials-based pH sensors for healthcare applications," *Prog. Mater. Sci.*, vol. 96, pp. 174–216, 2018.
[4] H. Lambers et al., "Natural skin surface pH is on average below 5, which is benefecial for its resident flora," *Int. J. Cosmetic Sci.*, vol. 28, pp. 359–370, 2006.
[5] T. J. Durkin, B. Barua, and S. Savagatrup, "Rapid detection of sepsis: Recent advances in biomarker sensing platforms," *ACS Omega*, vol. 6, pp. 31390–31395, 2021.
[6] A. P. Murphy and P. Rolfe, "Assessment of a commercial pH electrode used with blood," *J. Med. Eng. Technol.*, vol. 15, pp. 116–118, 1991.
[7] R. N. Khuri, S. K. Agulian, and R. I. Harik, "The liquid junction potential in blood pH determinations," *Phys. Med. Biol.*, vol. 13, 1968, Art. no. 23.
[8] D. J. Alner, J. J. Greczek, and A. G. Smeeth, "Precise standard pH values from 0 to 60°," *J. Chem. Soc. A.*, pp. 1205–1211, 1967.
[9] D. Choi et al., "A wearable potentiometric sensor with integrated salt bridge for sweat chloride measurement," *Sens Actuators B. Chem.*, vol. 250, pp. 673–678, 2017.
[10] H. Y. Y. Nyein et al., "A wearable electrochemical platform for noninvasive simultaneous monitoring of Ca2 and pH," *ACS Nano*, vol. 10, pp. 7216–7224, 2016.
[11] R. Wang et al., "Stretchable gold fiber-based wearable electrochem. sensor toward pH monitoring," *J. Mat. Chem. B.*, vol. 8, pp. 3655–3660, 2020.
[12] P. Chao, D. Ammann, U. Oesch, W. Simon, and F. Lang, "Extra-and intracellular hydrogen ion-selective microelectrode based on neutral carriers with extended pH response range in acid media," *Pflügers Archiv*, vol. 411, pp. 216–219, 1988.
[13] Y. Zhang et al., "Synthesis and biocompatibility assessment of PANI nanomaterials," *J. Bioact. Compatible Polym.*, vol. 34, pp. 16–24, 2019.
[14] Y. Tang et al., "Recent advances in wearable potentiometric pH sensors," *Membranes*, vol. 12, 2022, Art. no. 504.
[15] D. O'Hare, K. H. Parker, and C. P. Winlove, "Metal–metal oxide pH sensors for physiological application," *Med. Eng. Phys.*, vol. 28, pp. 982–988, 2006.
[16] R. A. Frederick, I. Y. Meliane, A. Joshi-Imre, P. R. Troyk, and S. F. Cogan, "AIROF electrodes for neural tissue stimul," *J. Neural Eng.*, vol. 17, 2020, Art. no. 056001.
[17] K. Chaisiwamongkhol, C. Batchelor, and R. G. Compton, ""pH sensing blood samples iridium for blood pH sensing," *Analyst*, vol. 144, pp. 1386–1393, 2019.
[18] J. Yang et al., "Digital pH test strips for in-field pH monitoring using iridium oxide-reduced graphene oxide hybrid thin films," *ACS Sensors*, vol. 1, pp. 1235–1243, 2016.
[19] K. Göbbels et al., "Neuronal cell growth on iridium oxide," *Biomaterials*, vol. 31, pp. 1055–1067, 2010.
[20] K. Izutsu and H. Yamamoto, "Iridium oxide pH-sensor in nonaqueous solution with other pH-Sensors," *Anal. Sci.*, vol. 12, pp. 905–909, Dec. 1996.
[21] X. Huang, Q. Ren, X. Yuan, W. Wen, W. Chen, and D. Zhan, "Iridium oxide based coaxial pH ultramicroelectrode," *Electrochem. Commm.*, vol. 40, pp. 35–37, 2014.
[22] M. E. Khakani, M. Chaker, and B. L. Drogoff, "Iridium thin films deposited by RF magnetron sputtering," *J. Vac. Sci. Tech. A.*, vol. 16, pp. 885–888, 1998.
[23] E. Slavcheva, R. Vitushinsky, W. Mokwa, and U. Schnakenberg, "Sputtered iridium oxide films as charge injection material for functional electrostimulation," *J. Elec. Soc.*, vol. 151, 2004, Art. no. E226.
[24] R. Y. Bekele et al., "CIGS sputtering targets fabricated from reclaimed materials," in *2013 IEEE 39th PVSC*, 2013, pp. 1938–1940.
[25] P. Savignac et al., "Improvement of adhesion properties and corrosion resistance of sol-gel coating on zinc," *Molecules*, vol. 23, 2018, Art. no. 1079.
[26] W. S. Al-Arjan et al., "Sol–gel preparation of well-adhered films of BaTiO3 and Bi2Ti2O7," *Mater. Res. Bull.*, vol. 74, pp. 234–240, 2016.
[27] X. Yang and J.-C. Chiao, "Integrated pH and sodium sensor array based on iridium oxide film," in *Proc. IEEE Sensors Conf.*, New Delhi, India, Oct. 2018, pp. 1–4.
[28] W. Huang et al., "A passive RF pH-Sensing tag for wireless food-quality monitoring," *IEEE Sensors J.*, vol. 12, no. 3, pp. 487–495, Mar. 2012.
[29] K. Chawang, S. Bing, and J.-C. Chiao, "Printable and flexible iridium oxide-based pH sensor by a roll-to-roll process," *Chemosensors*, vol. 11, 2023, Art. no. 267.
[30] H. R. Pohl, J. S. Wheeler, and H. E. Murray, "Sodium and potassium in health and disease," in *Interrelations Between Essential Metal Ions and Human Diseases*, Dordrecht, The Netherlands: Springer, 2013, pp. 29–47.
[31] Y. Liao and J. Chou, "Titanium dioxide thin films used for pH electrode and procaine drug sensor by sol–gel method," *Mater. Chem. Phys.*, vol. 114, pp. 542–548, 2009.
[32] D. H. Kim et al., "20-gauge ProCore needle in EUS-guided subepithelial tumor sampling: A prospective multicenter study," *BMC Gas.*, vol. 18, pp. 1–7, 2018.
[33] G. Geleto, W. Getnet, and T. Tewelde, "Mean vein diameter using sonography, southwest Ethiopia," *Ethiopian J. Health Sci.*, vol. 26, pp. 237–242, 2016.